Laboratory studies of field-aligned density striations and their relationship to auroral processes*

J. E. Maggs,† G. J. Morales, and W. Gekelman
University of California, Los Angeles, Los Angeles, California 90095-1696

(Received 13 November 1996; accepted 7 January 1997)

Magnetic field-aligned structures in current, density, and temperature are common features of the auroral ionospheric plasma. These structures both generate and transform low frequency waves in the plasma. The results of laboratory studies of two processes involving magnetic field-aligned density depletions (striations) that play a role in auroral plasma dynamics are presented. The first process involves the spontaneous generation of density and magnetic fluctuations at the striation edge. The nature of the fluctuations depends upon the electron plasma beta. At high beta (greater than the electron to ion mass ratio, m/M) the drift Alfvén wave is excited. At lower beta the density and magnetic field fluctuations separate and the shear Alfvén wave dominates. This process creates an environment conducive to electron acceleration along the magnetic field when the striation size is on the order of the electron skin depth because the shear Alfvén wave then has a substantial field-aligned electric field. The second process is the direct conversion of electromagnetic whistler waves to electrostatic lower hybrid waves at the striation edge. This process provides a mechanism for concentrating lower hybrid wave energy in the vicinity of striations where it may play a role in electron and ion heating. © *1997 American Institute of Physics.* [S1070-664X(97)91105-8]

I. INTRODUCTION

The dynamic auroral plasma is characterized by nonuniformities in density and magnetic field strength. One of the more striking and common of these nonuniformities is the magnetic field-aligned density depletion, or ''striation.'' Striations play a key role in the auroral ionosphere because they act as generators and transformers of wave energy. The density striations in the auroral ionosphere are characterized by a scale length across the magnetic field much smaller than the scale length along the magnetic field. Cross-field scale lengths for striations observed in the auroral ionosphere range from tens of meters to tens of kilometers while field aligned scale lengths range from hundreds to thousands of kilometers.[1]

In this paper we discuss the results of laboratory experiments involving the spontaneous generation of Alfvén waves by density striations, and the interaction of whistler waves with a density striation to produce lower hybrid waves. Both of these process play a role in the dynamics of the auroral ionosphere.

II. EXPERIMENT

The experiments discussed here were conducted in the Large Plasma Device (LAPD) at the University of California, Los Angeles.[2] The key to obtaining an understanding of the role of striations in plasma dynamics is the ability to produce an isolated striation in an otherwise uniform plasma under controlled conditions. A schematic of the LAPD illustrating the elements used in the formation and study of a controlled striation is shown in Fig. 1 together with a radial profile of the plasma density when a striation is present. The plasma is generated by electrons (primaries) emitted from a heated, barium–oxide coated cathode and subsequently accelerated by a semitransparent (transmission efficiency $\approx$50%) grid anode located 60 cm from the cathode. The accelerated primaries drift into a 9.4 m long vacuum chamber and strike neutral He gas at a fill pressure of $1-3\times10^{-4}$ Torr to generate a He^{+} plasma with a high degree (greater than 75%) of ionization. Typical plasma densities are in the range $n_e\approx1-4\times10^{12}$ cm^{-3}, with plasma electron temperature, $T_e\approx5-15$, eV, and estimated ion temperature $T_i\approx0.1-1$ eV. The axial magnetic field is varied from 0.5 to 2 kG.

Density striations are generated by two methods. The most ideal method consists of not applying the barium–oxide coating to a small spot ($\approx$1 cm radius) near the center of the nickel cathode so that primaries are not emitted from this region. Without primaries, plasma is not directly formed along field lines threading the spot and a density depletion results. The drawback to this method is that it does not allow for flexibility in striation parameters. The other method consists of placing a small copper disk supported on a long thin ($\approx$2 mm diam) ceramic shaft at a distance of 2 to 3 cm from a uniformly coated cathode. In this manner emission of primaries is suppressed and a density striation results along the field lines threading the disk. This technique results in density striations with properties nearly identical to those generated with the selective coating method, but the shaft introduces the undesirable feature of breaking the azimuthal symmetry of the striation. However, the processes reported here have been found to be unaffected by the method used to form the striation.

III. SPONTANEOUS GENERATION OF ALFVÉN WAVES

The spontaneous growth of magnetic and density fluctuations in the vicinity of a striation has been studied[3] for a

*Paper 6IA3, Bull. Am. Phys. Soc. **41**, 1502 (1996).
†Invited speaker.

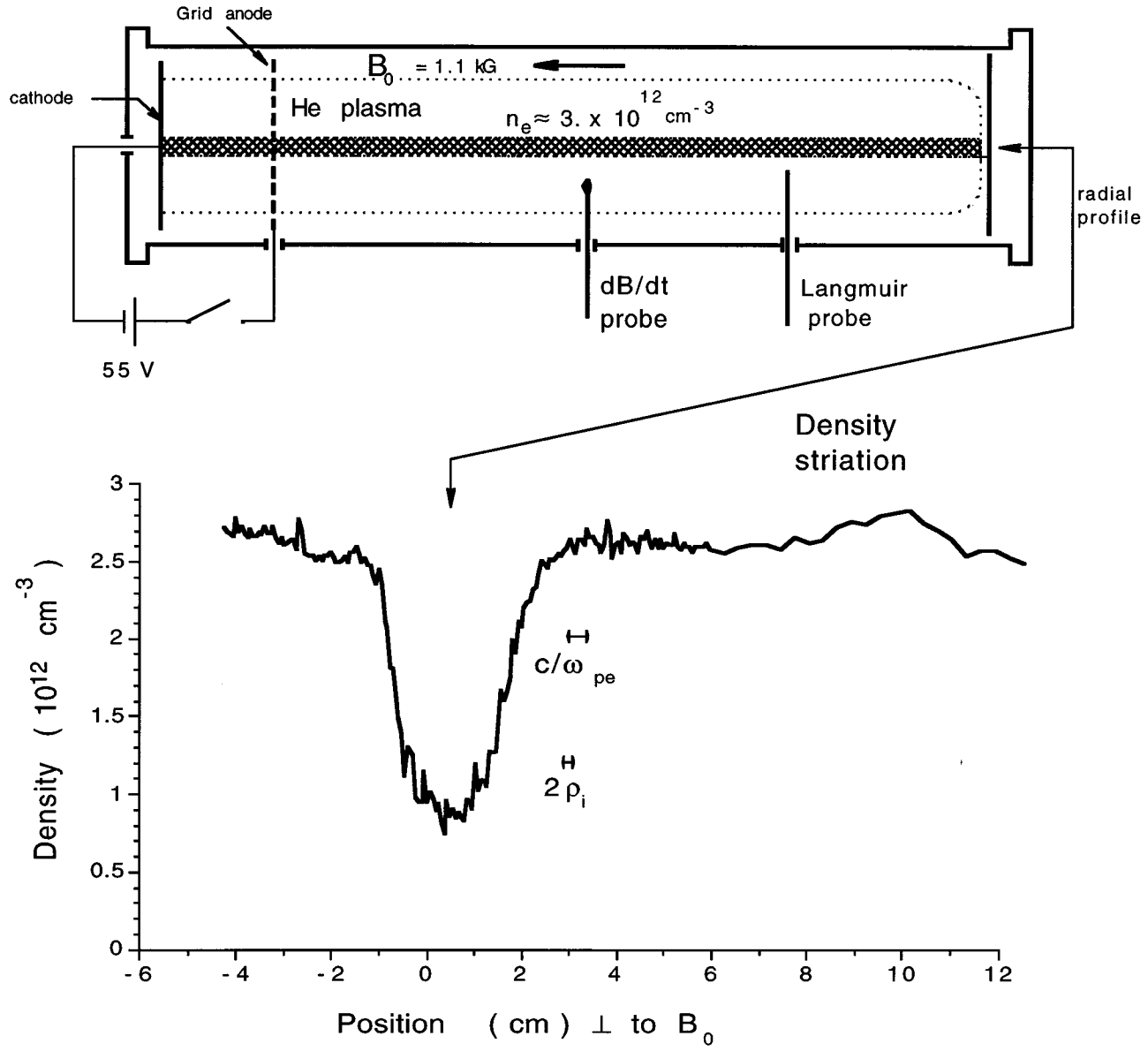

FIG. 1. A schematic of the geometry used in studying the spontaneous growth of magnetic fluctuations and a radial density profile through the center of the striation.

range of electron plasma betas, $\beta_e = 4\pi n T_e / B^2$, above and below the electron to ion mass ratio, m/M. The axial magnetic field is uniform and its strength is varied from 0.5 to 2 kG to produce a range of plasma betas. The density scale length across the magnetic field at the striation edge is typically, $L_n \approx 1$ to 2 cm, and the electron skin depth $c/\omega_{pe} \approx 5$ mm, the ion Larmor radius $\rho_i \approx 0.5-2$ mm, and the ion sound gyroradius $\rho_s = (T_e/M)^{1/2}/\Omega_i \approx 2-5$ mm. Hence, the ordering of spatial scales in these studies is $L_n \geqslant c/\omega_{pe} \geqslant \rho_s > \rho_i$.

The spontaneously generated magnetic fluctuations are measured with a small induction-loop probe consisting of mutually orthogonal coils (58 turns of 2.5 mm radius) in a triaxial arrangement. The global time evolution of the magnetic noise, $\delta B_\perp(t)$, detected by this probe in the neighborhood of the striation (at an axial position near the middle of the machine) is exhibited at the top of Fig. 2. The time evolution of the ion saturation current collected by a Langmuir probe is included for reference. The early part of the ion current trace indicates a buildup of plasma density. A steady state is obtained and held for about 1 ms after which the discharge current is terminated and the plasma density begins to decay. The detected magnetic signal is broadband while the amplitude is growing during the density buildup stage and eventually achieves a steady state consisting of low-frequency oscillations with frequencies about a tenth of the ion gyrofrequency, $f \approx 0.1 f_{ci}$ ($f_{ci} \equiv \Omega_i/2\pi$) as shown in the expanded view at the bottom of Fig. 2. After the discharge current is shut off, the magnetic fluctuations are found to decay while simultaneously decreasing their oscillation frequency. In subsequent discussions of the spectral properties of the fluctuations the time window for the Fourier transform corresponds to the 500 μs interval just prior to termination of the discharge during which steady state conditions prevail.

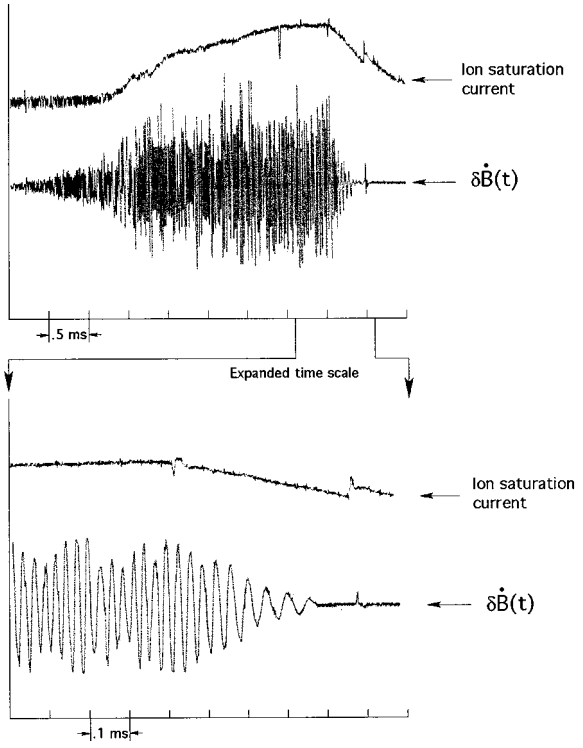

FIG. 2. The temporal evolution of ion saturation current and magnetic fluctuations with expanded detail around the end of the discharge phase of the plasma.

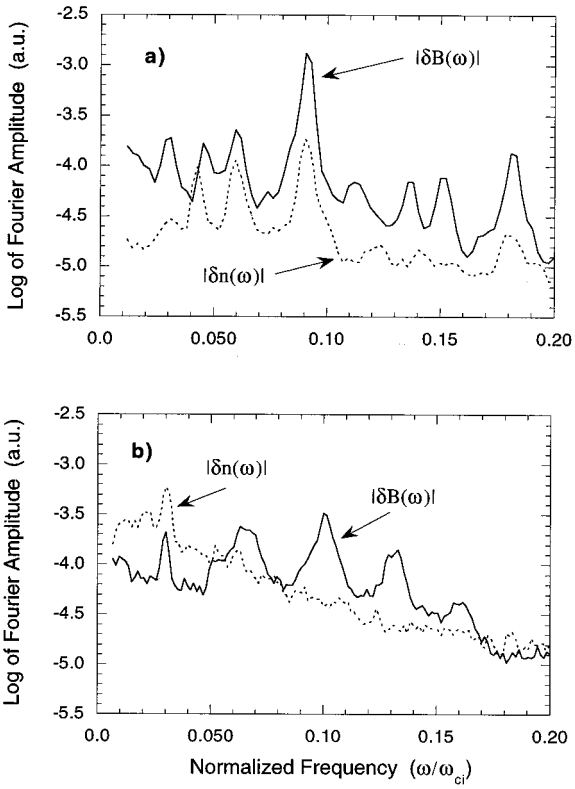

FIG. 3. The frequency spectra of magnetic fluctuations at (a) $\beta_e \approx 10^{-3}$ and (b) $\beta_e \approx 4.\times 10^{-4}$.

Measurements with a small Langmuir probe in the vicinity of the striation show that density fluctuations accompany the magnetic fluctuations. The fluctuations in density are obtained from the local ion saturation current which is proportional to $n_0(T_e/M)^{1/2}$. The local electron temperature can be determined from the current-voltage characteristic of the Langmuir probe, but this measurement is not fast enough to be used for correcting the ion saturation current for rapid fluctuations in T_e. Thus the signal referred to as a density fluctuation also contains contributions arising from fluctuations in the local electron temperature. Figure 3 exhibits the correspondence between the amplitude of the Fourier frequency transform of the density, $|\delta n(\omega)|$, and the magnetic field, $|\delta B(\omega)|$, for two different values of electron plasma beta, β_e. It is seen from Fig. 3(a) that at $\beta_e \approx 10^{-3}$ (>m/M) the fluctuations are coherent with a frequency spectra consisting of several sharp peaks resembling eigenfrequency spectra. In addition, an excellent correspondence exists between peaks in the density and magnetic spectra, particularly in the lower range of frequencies $\omega/\Omega_i < 0.1$. In this high β_e regime it is found from single-shot time traces that the oscillations in density and magnetic field are in phase. Figure 3(b) illustrates the behavior obtained as β_e is lowered to 3×10^{-4} (<m/M). It is seen that at this lower beta the signals are not nearly as coherent as at higher beta and the lines in the frequency spectra are broader. The correspondence between peaks in the density and magnetic spectra is limited to a small band $\omega/\Omega_i < 0.03$. For these conditions clear peaks exist in the magnetic fluctuations in the region $\omega/\Omega_i > 0.05$ where the density fluctuations exhibit an exponential frequency dependence.

The polarization of the magnetic fluctuations generated within the striation is extracted from the magnitude of the magnetic flux measured by each of the three mutually orthogonal coils that constitute the magnetic probe. It is found that the amplitude of the fluctuating magnetic field in the direction perpendicular to the background magnetic field, $|\delta B_\perp(\omega)|$, is much larger than the amplitude of the component parallel to the background field, $|\delta B_\parallel(\omega)|$. This observation indicates that the magnetic fluctuations are shear waves (as opposed to compressional waves).

Figure 4 displays the spatial dependence of the ambient plasma density, n_0, and the amplitude of the Fourier transform of the density fluctuations $|\delta n(\omega)|$ at a frequency cor-

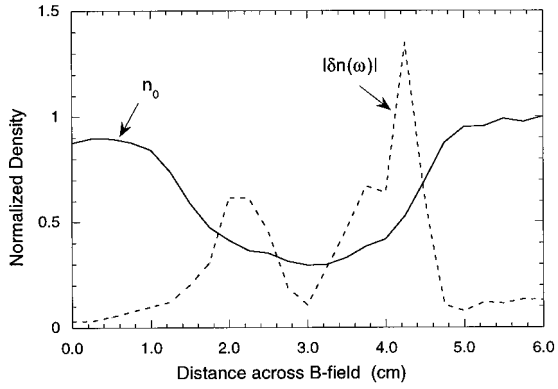

FIG. 4. A radial density profile in the vicinity of the striation with the amplitude of the Fourier frequency transform of the density fluctuations.

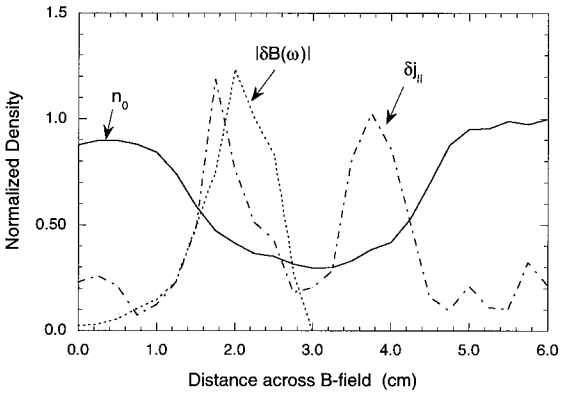

FIG. 5. The radial dependence of the rms field-aligned current fluctuations and the amplitude of the Fourier frequency transform of the perpendicular component of the magnetic fluctuations shown with a radial profile of the density.

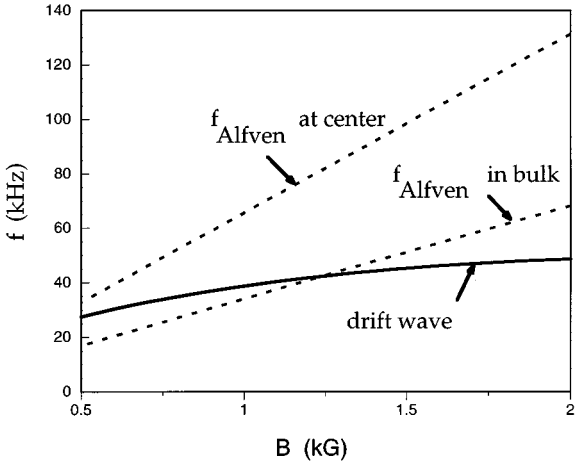

FIG. 6. The dependence with the background magnetic field strength of the drift wave frequency together with the Alfvén wave frequency inside and outside the striation for waves with parallel wavelengths twice the machine length.

responding to the peak in the spectra shown in Fig. 3(a), i.e., $\omega = 0.085\omega_{ci}$ (37 ± 2 kHz). For this case the contrast between the density in the center of the striation and the surrounding plasma is about a factor of 3. The radial profile of the amplitude of the Fourier transform of the magnetic field $|\delta B(\omega)|$ at a frequency of $0.085\omega_{ci}$ is shown in Fig. 5 where the ambient density profile is included for reference as in Fig. 4. The quantity $\delta j_{\parallel}$ also displayed in Fig. 5 is the rms value of the shot-to-shot fluctuations in the axial electric current measured using a double-sided Langmuir probe. The measurements of $|\delta B(\omega)|$ are shown only up to the center of the striation because the shielding and support structure of the magnetic probe is large enough to disturb the shape of the density profile if the probe is inserted through the striation. However, the $\delta j_{\parallel}$ profile is shown across the entire striation because the Langmuir probe is small enough not to significantly disturb the density profile. It is apparent in Figs. 4 and 5 that the density and magnetic fluctuations are trapped within the striation as would be expected for the radial profile of an eigenmode. The characteristic radial structure of the density and parallel current fluctuations exhibits a rough reflection symmetry about the center of the striation and the fluctuation amplitudes peak close to the point where the density gradient is maximum. The fact that the peak Fourier amplitude of the density fluctuation is higher on one side of the striation may be related to asymmetries in the striation density profile introduced by the shaft of the blocking disk.

Although both the density and magnetic fluctuations exhibit an eigenmode structure it is clear that a separation in the mode structure occurs as the value of β_e is changed. This separation can be understood from the theoretical boundaries shown in Fig. 6. The dashed lines in this figure bound the possible range of frequencies of shear Alfvén modes trapped within a density wave guide corresponding to the experimental parameters; one line corresponds to the Alfvén velocity at the center of the striation and the other to the value in the body of the plasma. As the confining magnetic field is increased the frequency of the pure Alfvén eigenmodes increases, as expected from the linear dependence of the Alfvén speed on magnetic field strength. The solid curve corresponds to the numerically obtained eigenfrequencies of electrostatic drift-waves trapped within the striation. Note the saturation behavior of the drift-wave eigenfrequencies as the magnetic field is increased. In a semiquantitative sense it is useful to think that the pure drift waves have a frequency related to the familiar local drift frequency $\omega = \omega_*/[1 + (k_\perp \rho_s)^2]$ with $k_\perp$ the perpendicular wave number, $\rho_s = (T_e/M)^{1/2}/\Omega_i$, and ω_* the electron diamagnetic drift frequency. Correspondingly the Alfvén eigenmodes approximately satisfy $\omega_A = \pi v_A/L$ where v_A is the Alfvén speed and L the length of the machine. The region in Fig. 6 for which the frequency of the Alfvén modes is smaller than the frequency of the drift waves defines the domain of drift-Alfvén eigenmodes, which for the experimental parameters corresponds to magnetic fields below 1.2 kG, and hence higher β_e. As the magnetic field is increased, and β_e subsequently lowered, the pure drift waves have a maximum frequency below 50 kHz, while the pure Alfvén eigenmodes separate and achieve higher frequencies, typically in the range 60–100 kHz. Indeed, the numerical values of the spectral peaks shown in Fig. 3 follow this classification. Those in Fig. 3(a) correspond to coupled magnetic and density fluctuations, that is, drift-Alfvén waves, while in Fig. 3(b) the lower band is associated with electrostatic drift waves and the higher frequencies are shear Alfvén waves.

Of all the various properties that we have measured, the best theoretical understanding has been achieved in the prediction of the eigenfrequencies and radial eigenmodes of the lower frequency modes that are well approximated by an electrostatic description. An example is given in Fig. 7, in which the solid curves represent analytical results and the open and dark symbols are measured quantities. The predicted frequency of the eigenmode is 38 kHz and the observed value is 37 ± 2 kHz. This theoretical prediction is based on a kinetic description that includes Lorentz collisions for electrons and whose details are the subject of a separate publication.[4] Another feature which is adequately represented by theoretical arguments is the separation of the

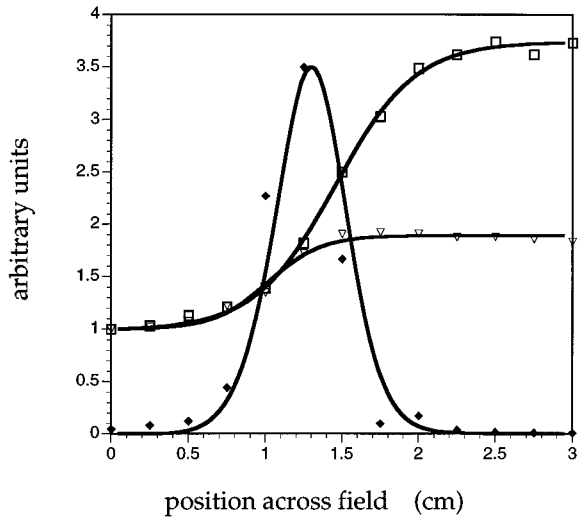

FIG. 7. A theoretical calculation of the radial profile expected for density fluctuations (solid lines) compared to measured values (diamonds) using smooth analytic approximations (solid lines) to measured density (squares) and temperature (triangles) profiles.

density and magnetic fluctuations at different values of β_e, as shown in Fig. 3. Overall the measurements are consistent with the criterion $\beta_e \approx$m/M for the separation between pure drift waves and Alfvén waves.

As illustrated in Fig. 2 the fluctuations rapidly disappear when the primary electron current is shut off and this behavior provides us with an opportunity to determine the driving source of the fluctuations. Two good candidates for the driving source are field-aligned currents and the cross-field pressure gradient. Five hundred microseconds after termination of the primary current the fluctuations are gone, but a substantial axial current carried by the bulk drift at about $0.1v_T$ has been observed to persist in the plasma while the plasma density profile shows no significant change. However, the most dramatic change is a substantial decrease in the electron temperature to about 3 eV everywhere in the plasma. The pressure difference across the striation drops by an order of magnitude mostly due to electron cooling. Since the fluctuations vanish when the primary current is terminated but the bulk axial current persists while the cross-field pressure gradient collapses, we attribute the driving source of the fluctuations to the cross-field pressure gradient.

In summary, we have reported the observation of substantial density and magnetic fluctuations ($\delta n/n_0 \approx 0.2$; $\delta B/B_0 \approx 2\times 10^{-3}$) arising spontaneously along a density striation in a laboratory plasma having many features in common with the auroral ionosphere. The fluctuations are trapped within the density striation and the radial structure of the fluctuations have scale sizes on the order of the cross-field gradient scale length. Density fluctuations can be strongly coupled to shearlike magnetic fluctuations depending upon the plasma beta. The laboratory observations have direct relevance to electron and ion acceleration process observed in the auroral ionosphere. However, in applying the results of the laboratory investigations, it should be kept in mind that the ratio of ion to electron temperature (T_i/T_e) in the laboratory plasma is probably smaller than that typically found in the ionosphere. Of particular interest to auroral dynamics are the shear Alfvén magnetic fluctuations which have an electric field along the magnetic field and may cause parallel electron acceleration. In this regard it is interesting to note that Alfvén waves have been associated with regions of auroral electron precipitation by rocket and satellite observations.[5] The Alfvén speed in the topside auroral ionosphere changes with altitude, initially increasing, reaching a peak between 0.5 and 1 R_E and then decreasing. The Alfvén speed at altitudes of 1 R_E corresponds to the velocity of keV electrons. Temerin, *et al.*[6] have proposed that this behavior of the Alfvén speed can lead to the acceleration of auroral electrons by Alfvén waves with cross-field scale sizes on the order of the electron skin depth. The parallel electric field associated with the shear Alfvén wave[7] depends upon the ratio of the perpendicular wave length, $2\pi/k_\perp$, to the electron skin-depth and is largest for $k_\perp c/\omega_{pe} \approx 1$. Thus the largest parallel electric fields should be associated with scale lengths on the size of the electron skin-depth which scales very well with the thickness of discrete auroral arcs.[8] In addition the spatial localization of the perpendicular electric field arising from confinement of the wave by the striations can lead to ion heating.[9] Such ion heating associated with density striations has been observed by rocket and satellite in the auroral ionosphere.[10]

IV. WHISTLER WAVE INTERACTION WITH STRIATIONS

A second process of interest to the dynamics of the auroral ionosphere involves the interaction of electromagnetic whistler waves with striations having cross-field scale sizes smaller than the whistler wavelength. In this situation the whistler wave interaction with the striation results in the direct conversion[11] of the electromagnetic whistler wave into electrostatic lower hybrid waves at the striation boundary.[12] This process has been observed with satellites to occur in the auroral ionosphere.[13] In the direct conversion process incident electromagnetic whistler waves with parallel wave number, $k_\parallel$, produce several product waves with the same $k_\parallel$, but different values of $k_\perp$ since multiple values of $k_\perp$ are allowed by the dispersion relation. A broad spectrum of perpendicular wave numbers, $\Delta k_\perp$, is provided by the striation density gradient. This spectrum of $\Delta k_\perp$ values allows the jump from one mode to the other. It is important to note that the spectrum is limited by the steepness of the gradient. The smoother the gradient, the smaller the gap which can be bridged in $k_\perp$. For frequencies between the lower hybrid resonance and half the electron cyclotron frequency, $f_{\mathrm{LH}} < f < f_{ce}/2$, the cold plasma dispersion relation allows up to four values of $k_\perp$ for any $k_\parallel$ corresponding to a whistler wave. Thus, the incident wave potentially can linearly couple to one whistler and one lower hybrid mode inside, and one whistler and one lower hybrid mode outside the striation.

In the laboratory studies of the interaction process,[12] a striation with a 6 cm diameter and central density of 3×10^{11} cm^{-3} is created in an 80 cm diameter He plasma column of density 9×10^{11} cm^{-3} with a 480 G axial magnetic field. The incident whistler wave is launched in a quasicontinuous fashion (several thousand cycles) at a frequency of 101 MHz

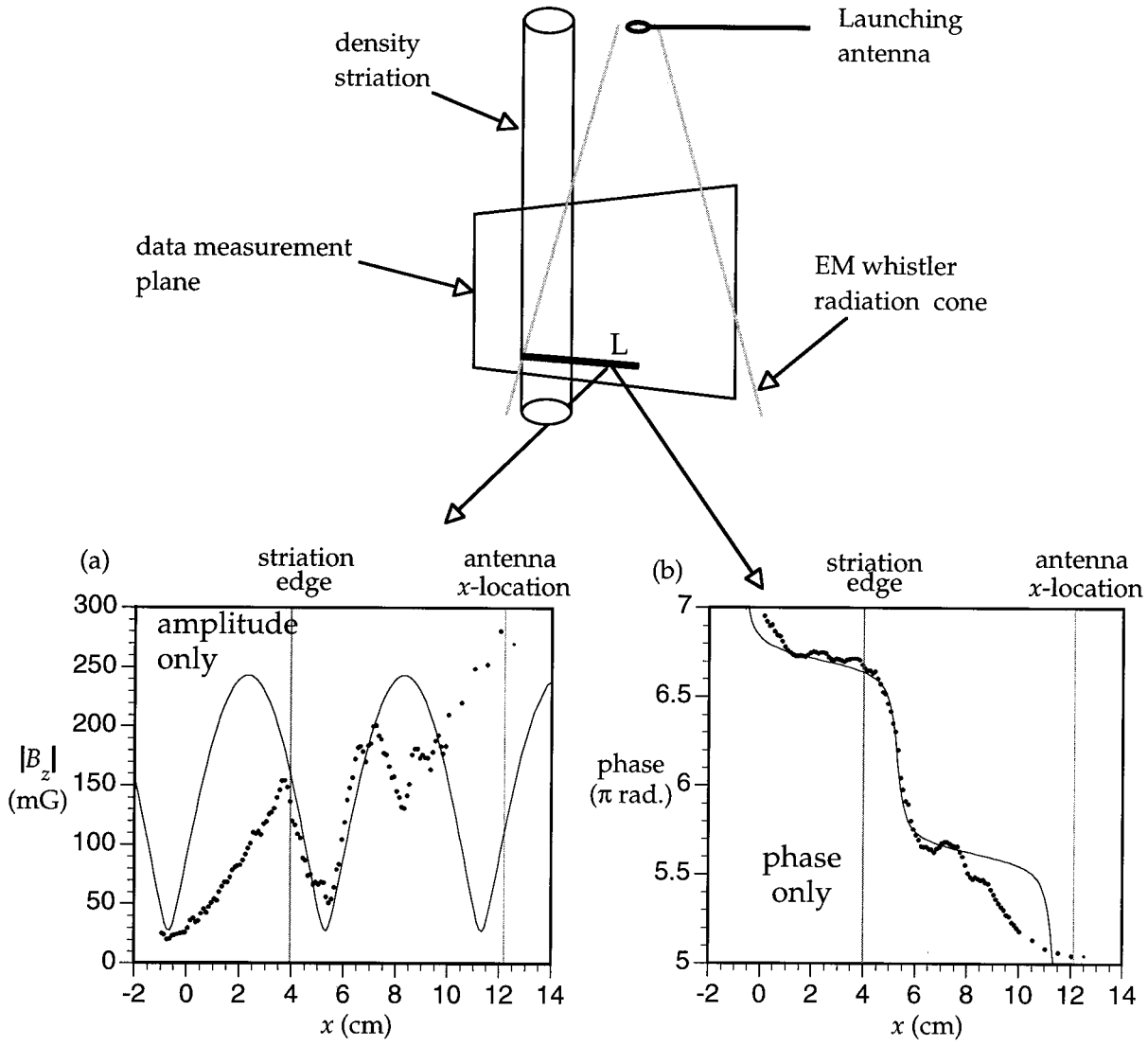

FIG. 8. A schematic of the geometry used in the whistler–striation interaction experiment showing the relative location of the measurement plane, striation, and launching antenna together with the (a) measured wave amplitude and (b) phase.

by a 2 cm diam loop antenna completely insulated with glass from the plasma in order to ensure purely inductive coupling. The loop antenna is oriented with its normal parallel to the background magnetic field, B_0. The size and inductive nature of the antenna allow it to couple efficiently to electromagnetic whistler waves. It was confirmed by direct measurement in a uniform plasma that the antenna radiates only electromagnetic whistler waves and produces no short wavelength electrostatic lower hybrid radiation. The density gradient at the striation edge is very sharp with the minimum gradient scale length, $L_{\nabla} \equiv N_e/\nabla N_e$, almost 1.5 cm which is on the order of 0.1 of the launched whistler perpendicular wavelength.

The geometry of the experiment is illustrated at the top of Fig. 8. The launching antenna is located 15 cm from the striation edge and about 2 cm below its center. Data is taken on a roughly rectangular 30×35 cm grid through the center of the striation at about 4000 points. Figure 8(a) shows the amplitude of the component of the wave magnetic field parallel to the background magnetic field, B_z, and Fig. 8(b) shows the phase of B_z measured relative to the launched wave along a representative line, L, in the data plane. The most striking feature of Fig. 8(b) is a 180° phase shift, in the perpendicular direction, which occurs at $x \approx 5$ cm, over a space of only 1 cm. The phase shift also corresponds to a marked amplitude minimum which runs parallel to the striation edge at $x = 5.5$ cm. These characteristics indicate that superposition of the incident whistler waves with reflected whistler waves is taking place in the vicinity of the striation boundary. The expected behavior of an incident whistler wave with perpendicular wave number 0.53 cm^{-1} superposed with a reflected whistler of the same wave number but 80% of the amplitude is shown by the solid lines in Figs. 8(a) and 8(b). The close agreement between the measured data and the expected behavior for the superposed wave in the range between 4 cm $< x <$ 8 cm indicates the production of reflected whistlers during the interaction.

Evidence of short wavelength structure near the striation edge can be seen in Fig. 8(b) as short wavelength fluctuations in the phase in the region around the striation edge at 1

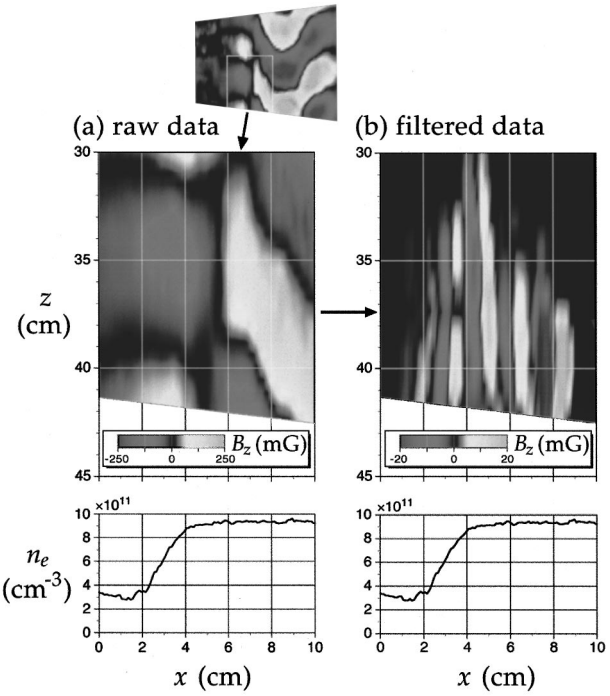

FIG. 9. An overall grayscale view of the B_z component of the wave field in the measurement plane is shown in detail near the striation, (a) without filtering for the short wavelength and (b) with filtering. Radial density profiles of the striation are shown below each detail to aid in orientation.

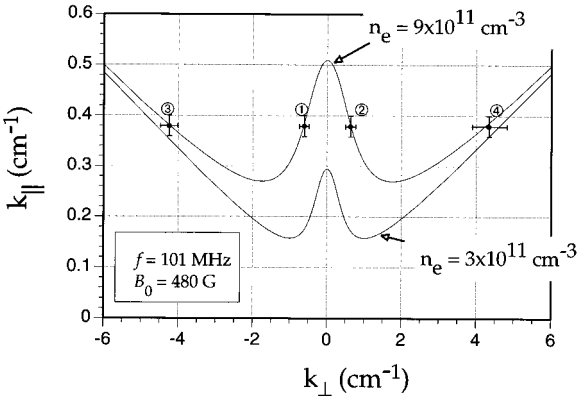

FIG. 10. Wave number surfaces ($k_\perp$ vs $k_\parallel$) are shown for the plasma at the striation center and in the bulk plasma together with the measured values of the wave numbers for the ① incident whistler, ② reflected whistler, ③ converted lower hybrid wave in the bulk plasma, and ④ converted lower hybrid wave in the striation.

cm $< x <$ 10 cm. This short wavelength structure is not very apparent in the magnetic data because the lower hybrid wave is nearly electrostatic in nature and possess a relatively small magnetic component. Nonetheless the short wavelength structure can be extracted from the magnetic data using a filtering process. Figure 9 shows the raw data in the interaction region which are magnified in Fig. 9(a) and the filtered data in this same region are shown in Fig. 9(b). Dark grays indicate negative values of B_z and light grays indicate positive values of B_z. Black indicates a zero value of B_z. Figure 9(b) shows that the phase fronts of the short wavelength lower hybrid waves are nearly, but not exactly, aligned with the background magnetic field. A close examination reveals that, on either side of the striation boundary, at $x=4$ cm, the phase fronts are angled such that their corresponding wave vectors point toward the boundary with a very small component pointing along the background magnetic field. Thus, the reflected and transmitted lower hybrid waves propagate towards each other as expected for the ''backwards propagating'' (in the perpendicular direction) lower hybrid wave. The energy of these waves, on the other hand, radiates primarily along the background magnetic field with a small component away from the striation boundary.

From a detailed analysis of the peak and trough data underlying Fig. 9 typical perpendicular and parallel wave numbers are calculated for the lower hybrid waves. The results are shown in Fig. 10 which displays the measured wave numbers compared to wave normal surfaces computed from the cold plasma dispersion relation inside and outside the striation. The upper curve is calculated for the density outside the striation, 9×10^{11} cm^{-3}, and the lower curve is for the minimum density within the striation, 3×10^{11} cm^{-3}. The combined ($k_\perp$, $k_\parallel$) of the four observed wave modes are plotted as points labeled ①–④. Modes ①–③, the whistler waves and a lower hybrid wave generated by direct conversion, propagate outside the striation in the high density region. As such, they are expected to lie on the upper curve which, in fact, they do with great accuracy. The difference between the predicted and observed values is less than 1%, well within the experimental error of, typically, $\pm$5% for these modes. Mode ④ is the lower hybrid wave generated by direct conversion that propagates within the striation boundary region where the density changes over a very short distance. Its $k_\perp$ is expected to lie somewhere between the high and low density curves, 4.5 cm^{-1} for example, which corresponds to a density halfway between the two extremes. The observed value is much closer to the high density curve at 4.3 cm^{-1}. However, the error associated with its measurement is large enough to include the entire range between the two curves.

The direct conversion process of electromagnetic whistlers into lower hybrid waves is of interest in the auroral ionosphere because lower hybrid waves have been observed on rocket flights to be associated with ion heating and density striations.[10] The commonly held belief that the process of lower hybrid collapse was responsible for this association has been called into question by Pecseli *et al.*[14] whose observations also indicate that lower hybrid waves may play a key role in the production and maintenance of striations due to refractive focusing of these waves. The direct conversion process of electromagnetic whistler waves into lower hybrid waves has been inferred to occur in the presence of ionospheric striations from satellite observations of ground launched VLF waves.[13] The laboratory measurements confirm the direct conversion process[12] and thus indicate that electromagnetic whistlers, perhaps those produced by lightning, may account for some of the lower hybrid waves observed associated with ionospheric striations.

V. CONCLUSIONS

Plasma processes that occur in space can be reproduced and studied in the laboratory. Experimental studies in the laboratory and space are often complementary. Laboratory studies can provide detailed information on the spatial structure and temporal evolution of these processes, information that is often difficult or impossible to obtain from spacecraft measurements. Spacecraft observations often provide detailed information on plasma electron and ion velocity space distributions which are difficult to obtain in the laboratory. Thus a great deal of progress towards obtaining a quantitative understanding of the important plasma physical processes that govern space plasma dynamics can be achieved by coordinated studies involving laboratory and space observations.

ACKNOWLEDGMENTS

The whistler direct conversation research constitutes the Ph.D. thesis work of J. Bamber. We thank J. Peñano and D. Leneman for valuable contributions to the work on drift-Alfvén waves.

This research is sponsored by the Office of Naval Research and the National Science Foundation.

[1] D. H. Clark and W. J. Raitt, Planet. Space Sci. **24**, 873 (1976); P. L. Dyson, J. Geophys. Res. **74**, 6291 (1969); B. G. Fejer and M. C. Kelley, Rev. Geophys. Space Phys. **18**, 401 (1980).

[2] W. Gekelman, H. Pfister, Z. Lucky, J. Bamber, D. Leneman, and J. Maggs, Rev. Sci. Instrum. **62**, 2875 (1991).

[3] J. E. Maggs and G. J. Morales, Geophys. Res. Lett. **23**, 633 (1996); Phys. Plasmas **4**, 290 (1997).

[4] J. R. Peñano, G. J. Morales, and J. E. Maggs, Phys. Plasmas **4**, 555 (1997).

[5] R. Lundin, L. Eliasson, G. Herendel, M. Boehm, and B. Holback, Geophys. Res. Lett. **21**, 1903 (1994); M. H. Boehm, C. W. Carlson, J. P. McFadden, J. H. Clemmons, and F. S. Mozer, J. Geophys. Res. **95**, 12157 (1990); K. Stasiewicz, G. Gustafsson, G. Marklund, P.-A. Lindqvist, J. Clemmons, and L. Zanetti, J. Geophys. Res. **102**, 2565 (1997).

[6] M. Temerin, J. McFadden, M. Boehm, C. W. Carlson, and W. Lotko, J. Geophys. Res. **91**, 5769 (1986).

[7] G. J. Morales, R. S. Loritsch, and J. E. Maggs, Phys. Plasmas **1**, 3775 (1994).

[8] J. E. Borovsky, J. Geophys. Res. **98**, 6101 (1993).

[9] K. J. Reitzel and G. J. Morales, Phys. Plasmas **3**, 3251 (1996).

[10] G. P. Garbe, R. L. Arnoldy, T. E. Moore, P. M. Kintner, and J. L. Vago, J. Geophys. Res. **97**, 1257 (1992); J. L. Vago, P. M. Kintner, S. W. Chesney, R. L. Arnoldy, K. A. Lynch, T. E. Moore, and C. J. Pollock, *ibid*. **97**, 16935 (1992); R. E. Erlandson, L. J. Zanetti, M. H. Acuna, A. I. Eriksson, L. Eliasson, M. H. Boehm, and L. G. Blomberg, Geophys. Res. Lett. **21**, 1855 (1994).

[11] A. Y. Wong, G. J. Morales, D. Eggleston, J. Santoru, and R. Behnke, Phys. Rev. Lett. **47**, 1340 (1981); G. J. Morlaes, S. N. Antani, and B. D. Fried, Phys. Fluids **28**, 3302 (1985).

[12] J. F. Bamber, J. E. Maggs, and W. Gekelman, J. Geophys. Res. **100**, 23795 (1995).

[13] T. F. Bell and H. D. Ngo, J. Geophys. Res. **95**, 149 (1990); T. F. Bell, H. G. James, U. S. Inan, and J. P. Katsufrakis, *ibid*. **88**, 4813 (1983).

[14] H. L. Pecseli, K. Iranpour, Ø. Holter, B. Lybekk, J. Holtet, J. Trulsen, A. Eriksson, and B. Holback, J. Geophys. Res. **101**, 5299 (1996).